Characterization of Single-Port SAW Resonators at 3.7 GHz Based on Epitaxial $LiNbO_3$ Layers

Alexandre Clairet, Stefania Oliveri, Anthony Almirall, Thomas Baron, William Daniau, and Ausrine Bartasyte
FEMTO-ST Institute, UBFC, CNRS, ENSMM
Time and Frequency department
Besançon, France
Email: alexandre.clairet@femto-st.fr

Abstract—**The performance of single-port surface acoustic wave resonators based on 150 nm thick Z-axis oriented $LiNbO_3$ films on C-sapphire was studied by means of simulations. The resonance frequencies close to 3.7 GHz were targeted. The dependence of wave velocity and electromechanical coupling on the propagation direction was determined. Effects of a presence of 60° growth domains in films, or changes in Li composition in $LiNbO_3$ layers and thicknesses of piezoelectric film and electrodes on the SAW properties was evaluated theoretically, as well.**

Keywords— $LiNbO_3$; thin films; SAW; high frequency;

I. INTRODUCTION

$LiNbO_3$ (LN) single crystals are widely used for the surface acoustic wave (SAW) devices such as radio frequency (RF) filters and sensors due especially its high electromechanical coupling factor, k^2. Its k^2 is around 5 % for a Rayleigh wave and higher than 10 % for a pseudo-SAW (PSAW), also known as Leaky SAW [1]. To be applied, SAW devices must have low insertion losses and a pure spectral signature. In the case of RF filters, low temperature coefficient of frequency (TCF) and high electromechanical coupling count, as well. So far the frequency of SAW devices based on single crystal technology is limited to the 3.5 GHz. Next generation applications of SAW devices demands operational frequencies at least up to 6 GHz. There are two possibilities to increase the SAW frequency: a creation of guided acoustic waves in the heterostructures and/or a reduction of the period of interdigital transducers (IDTs). However, deep UV lithography is already used at its resolution limits. The possibility to accelerate SAW have been demonstrated theoretically and experimentally for LN films on sapphire or diamond substrates, in which propagation velocities are higher than in LN single crystals [2-4]. In literature, Z-axis oriented epitaxial growth of LN films is the most frequently studied one. The propagation velocities and electromechanical coupling along X- and Y- axis as a function of thickness of Z-LN films on C-sapphire substrates have been estimated by means of simulations and have been confirmed experimentally. It has been shown that these two propagation directions presented different acoustic responses. Little is known about acoustical propagation along other directions in this heterostructure. The as-grown films usually present 60° oriented growth domains, which can be eliminated by growing or annealing films at high-temperature (around 800 °C) [2]. However, at these temperatures Li_2O volatility from films is considerable. The acoustic velocity in $LiNbO_3$ depends on the Li nonstoichiometry, as well. Thus, uncontrolled Li_2O volatility may result in difficulties to reproduce the operational frequencies of acoustical devices based on LN films. In order to optimize the acoustical performance of grown of Z-LN films, it is worth knowing in advance if the presence of 180° domains impacts the propagation properties and if the change of Li nonstoichiometry induces significant modification of frequency.

In this work the complete angular dispersions of propagation velocities and electromechanical coupling were determined numerically for Z-LN films on C-sapphire substrates in order to evaluate the possible effect of the presence of 60 ° growth domains in films. Finite element analysis was used to estimate the effect of Li nonstoichiometry on the acoustical response (frequency, k^2, and TCF) of single-port SAW resonator operating at 3.7 GHz and to compare the compositional effect to the possible fabrication imprecisions (variations in the thicknesses of the piezoelectric film and IDTs).

II. EXPERIMENTAL DETAILS

The main epitaxial relationship of Z-LN films with C-sapphire (Sapp) substrate is $(0001)_{film}||(0001)_{Al2O3}$ and $[11\bar{2}0]_{film}||[11\bar{2}0]_{Al2O3}$ (matrix) and the 60° growth domains present $[11\bar{2}0]_{film}||[\bar{1}\bar{1}20]_{Al2O3}$. According to IEEE convention [5], these two orientations can be named as LN(ZXt)/ψ//Sapp(ZXt)/ψ and LN(ZXt)/ψ+60° // Sapp(ZXt)/ψ. The heterostructure composed of 150 nm thick Z-LN film on C-sapphire substrate was considered in this study. In order to find out theoretically k^2, TCF and resonant frequencies of single-port SAW resonators, 1D and 2D simulations were performed by combined finite element (FEM)/boundary element analysis [5]. The single-port resonator consisted of sixty aluminum IDT pairs and twenty aluminum mirrors on each side of resonator. The thickness of Al and the SAW wavelength were set to 100 nm and 1.4 µm, respectively. Four propagation directions, ψ, in LN films were considered: (ZXt)/0°, (ZXt)/30°, (ZXt)/60°, and (ZXt)/90°. The elastic, piezoelectric and dielectric constants of congruent LN were taken from Kovacs et al. [6] and the equivalent constants for stoichiometric LN were estimated from Kushibiki et al. data

This work was supported by French National Research Agency fundings ANR LiLit (ANR-16-CE24-0022-011), ANR JCJC LiLa (ANR-12-JS04-0008-01), Labex ACTION program (ANR-11-LABX-0001-01), the French RENATECH network, and FEDER Research Grant No. FC0001257-11002 with SMART-INN project.

[7]. The possible variations in thicknesses of electrodes and piezoelectric film were assumed to be ± 5 nm.

III. Results

A. 1D simulations

The dependence of effective permittivity, ε_{eff}, on propagation velocity in Al/LN(ZXt)/0°/Sapp(ZXt)/0° stack (propagation direction is along X-axis), obtained by 1D simulations, is presented in Fig.1. There were observed two SAW modes with v = 4845 m/s (wave ♯1) and v = 5256 m/s (wave ♯2) with purely real effective permittivity. The frequencies of these modes were 3.46 GHz and 3.75 GHz, respectively. These two surface acoustic waves with v = 4906 m/s (f = 3.50 GHz) and v = 5174 m/s (f = 3.70 GHz) were also observed for the LN(ZXt)/60°/Sapp(ZXt)/0° configuration. The change of the wave velocity of these two modes in LN(ZXt)/0°/Sapp(ZXt)/0° and LN(ZXt)/60°/ Sapp(ZXt)/0° heterostructures as a function of propagation direction ($0° \leq \psi \leq 360°$) is illustrated in Fig. 2 a. In the case of LN film matrix and 180° growth domains the angular dispersions of wave velocities and k^2 presented six-fold symmetry. This indicated that the propagation properties along X (Y) and –X (-Y) axes were equivalent. In the case of both growth orientations, the wave ♯2 vanished and wave ♯1 accelerated when propagation direction was parallel to Y or –Y axes ($\psi = 30 + 60n$, where n is integer). The velocity of the wave ♯2 was highest when it propagated along X or –X axes ($\psi = 0 + 60n$). The angular dispersion of velocities of both waves was reduced in LN(ZXt)/60°/Sapp(ZXt)/0° growth domains compared to that of LN(ZXt)/0°/Sapp(ZXt)/0° matrix. In the case of wave ♯1, the minimum value of the velocity was increased from 4845 m/s to 4907 m/s in the 60 °- domains while its maximum value was similar for the both growth orientations. Accordingly, the maximum velocity of wave ♯2 changed from 5280 m/s to 5175 m/s in the secondary orientation.

The change of the electromechanical coupling factor of wave ♯1 and wave ♯2 in LN(ZXt)/0°/Sapp(ZXt)/0° and LN(ZXt)/60°/Sapp(ZXt)/0° heterostructures as a function of propagation direction ($0° \leq \psi \leq 360°$) is presented in Fig. 2 b. In the case of wave ♯2, k^2 was increased by more than a factor of two in 60°-domains (4.25 %) compared to that in the film matrix (1.9 %). The highest k^2 of this wave was observed at $\psi = 0 + 60n$ in both growth orientations. The wave ♯1

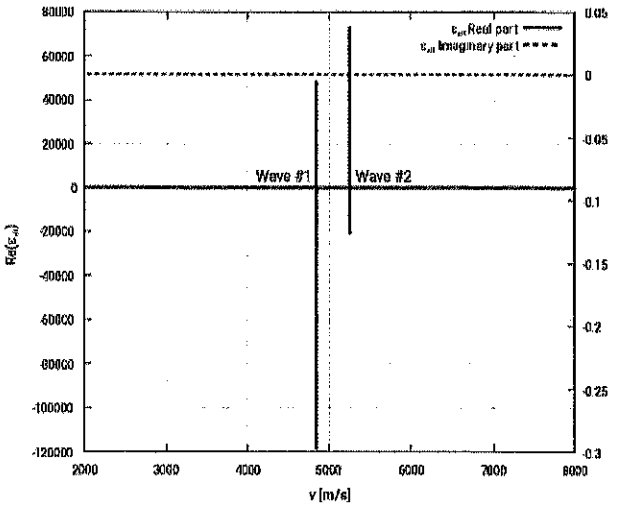

Fig. 1. Real and imaginary parts of the effective permittivity as a function of wave velocity, determined for the stack of 100 nm Al/150 nm $LiNbO_3$ /sapphire.

propagating in LN(ZXt)/0°/Sapp(ZXt)/0° and LN(ZXt)/60°/ Sapp(ZXt)/0° heterostructures presented maxima of k^2 at $\psi = 0 + 60n$ and $\psi = 30 + 60n$, respectively.

B. 2D simulations

2D simulations by using the FEM/boundary element analysis were done for two main propagation directions, ψ = 0° and 90°, and two growth orientations: LN(ZXt)/0°// Sapp(ZXt)/0°, LN(ZXt)/90°//Sapp(ZXt)/90°, LN(ZXt)/60°// Sapp(ZXt)/0°, and LN(ZXt)/150°//Sapp(ZXt)/90°. The frequency dependence of complex admittance of the studied single-port resonator was determined for each configuration. The Fig. 3 shows frequency function of the real part of the admittance – conductance, G. One can note that SAW velocity was considerably modified when wave propagated along X-axis in 60°- domains compared to the propagation in the matrix, while the SAW propagating along Y-axis was not affected (identical conductance) by the 60 ° rotation of the LN lattice with respect to the sapphire one. The SAW resonator based on LN(ZXt)/0°// Sapp(ZXt)/0° presented single resonant frequency at 3.49 GHz (v = 4884 m/s). This velocity was close

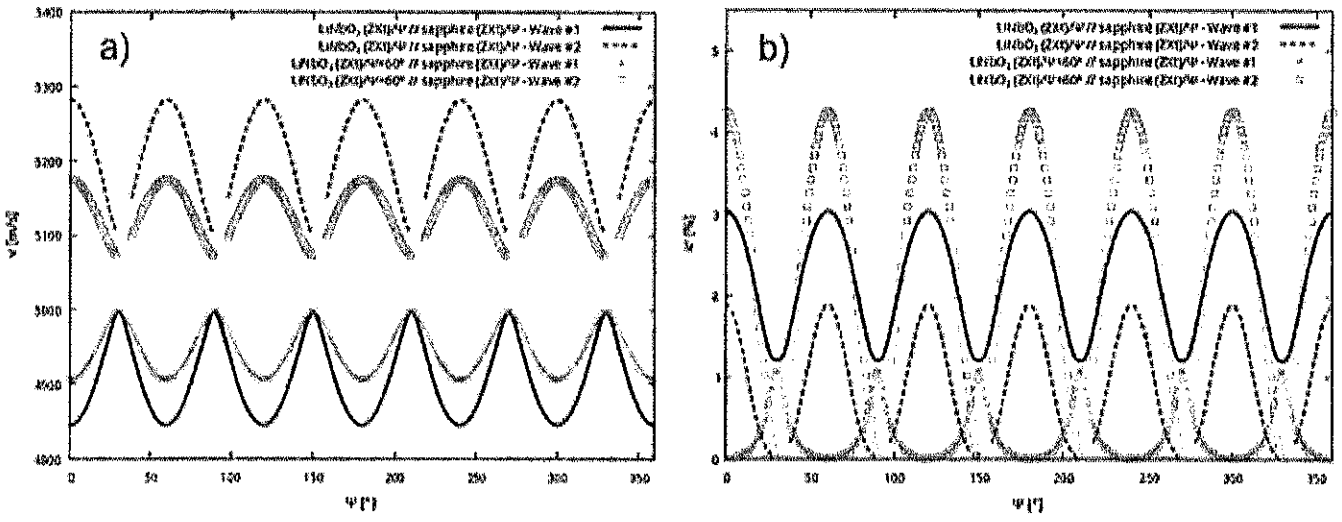

Fig. 2. Wave velocity, v, (a) and electromechanical coupling factor, k^2, (b) as a function of propagation direction, ψ, of wave ♯1 and wave ♯2 for the two crystalline growth orientations: $LiNbO_3$ (ZXt)/ψ // sapphire (ZXt)/ψ (solid and dashed lines) and $LiNbO_3$ (ZXt)/ψ + 60° // sapphire (ZXt)/ψ (curves with crosses and squares).

to that of the wave #1 (v = 4845 m/s), predicted by means of 1D simulations. In the case of both LN(ZXt)/90°// Sapp(ZXt)/90° and LN(ZXt)/150°// Sapp(ZXt)/90° (matrix and 60°-domains, respectively) structures, the wave #1 was observed with frequency of 3.58 GHz (v = 5015 m/s) while the wave #2 was not present again. Finally, the SAW frequency response simulated for the LN(ZXt)/60°// Sapp(ZXt)/0° configuration showed a resonance at 3.638 GHz (v = 5093 m/s) which could correspond to the wave #2 according to 1D analysis.

To summarize, the presence of 60° growth domains may significantly affect operational frequency and electromechanical coupling of SAW devices based on epitaxial Z-LN layers on C-sapphire. It is important to note that this theoretical analysis was not able to predict the frequency response of the mixture of the two growth orientations.

We would like to stress that the difference in the theoretical and experimental frequencies of SAW devices based on LN films may have different origin than the presence of growth domains and might be related to: (i) imprecision in thicknesses of piezoelectric and/or electrode layers; (ii) difference in Li nonstoichiometry; (iii) presence of residual stresses; (iv) etc. The effect of change in thickness of LN (hLN) and Al (hAl) layers on the propagation velocity, electromechanical coupling and TCF is summarized in the Table I. In general, the wave velocity decreased and k^2 increased with the increase of LN thickness. The thicker Al electrodes (+ 5 nm) resulted in the faster propagation and ameliorated coupling of SAW resonators. The drift of frequency with temperature increased for thicker Al and LN layers. Li nonstoichiometry effect on the propagation velocity seemed to be minor as velocity in stoichiometric LN/sapphire heterostructure was calculated to be lower only by 10 m/s than in the congruent LN/sapphire.

TABLE I. EVOLUTION OF THE WAVE VELOCITY, COUPLING FACTOR, AND TCF AS A FUNCTION OF LN AND Al FILM THICKNESSES

SAW configuration	Parameter	v [m/s]	k^2 [%]	TCF [ppm/°C]
0° // 0°	Reference	4884	3.65	-72.7
	$LiNbO_3$ - 5 nm	4900	3.47	-72.0
	$LiNbO_3$ + 5 nm	4864	3.81	-73.2
	Al - 5 nm	4913	3.48	-70.3
	Al + 5 nm	4848	3.74	-74.6
90° // 90°	Reference	5015	5.51e-2	
	$LiNbO_3$ - 5 nm	5037	4.80e-2	
	$LiNbO_3$ + 5 nm	4985	6.23e-2	
	Al - 5 nm	5064	5.46e-2	
	Al + 5 nm	4963	5.57e-2	
60° // 0°	Reference	5093	2.03e-2	-73.9
	$LiNbO_3$ - 5 nm	5110	1.35e-2	-73.3
	$LiNbO_3$ + 5 nm	5075	2.04e-2	-74.5
	Al - 5 nm	5127	0.67e-2	-71.3
	Al + 5 nm	5054	3.42e-2	-76.0
150° // 90°	Reference	5015	4.82e-2	
	$LiNbO_3$ - 5 nm	5037	4.11e-2	
	$LiNbO_3$ + 5 nm	4990	5.54e-2	
	Al - 5 nm	5064	5.45e-2	
	Al + 5 nm	4963	5.57e-2	

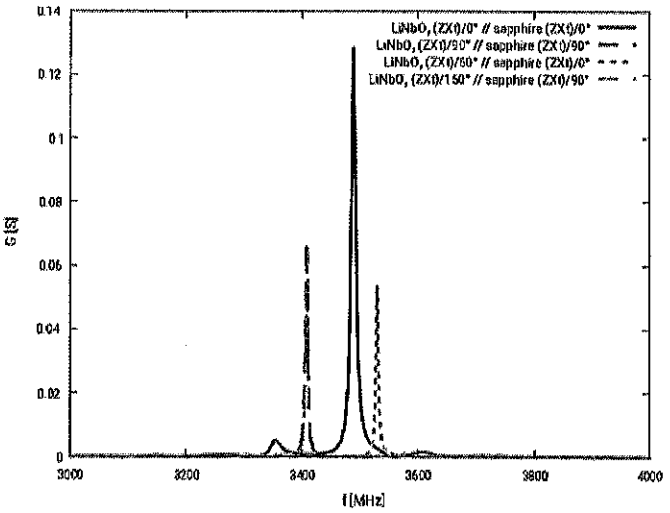

Fig. 3. Conductance, G, as a function of frequency for the four SAW configurations: LN(ZXt)/0°// Sapp(ZXt)/0°, LN(ZXt)/90°//Sapp(ZXt)/90°, LN(ZXt)/60°// Sapp(ZXt)/0°, and LN(ZXt)/150°//Sapp(ZXt)/90°.

IV. CONCLUDING REMARKS

It was shown by 1D and 2D FEM/boundary element analysis that the presence of 60° growth domains might significantly affect operational frequency and electromechanical coupling of SAW devices based on epitaxial Z-LN layers on C-sapphire. Li nontsoichiometry effect on the acoustic propagation properties (k^2, TCF and frequency) seemed to be negligible as compared to the possible imprecisions and inhomogeneity of the thicknesses of piezoelectric layer and IDTs.

ACKNOWLEDGMENT

We are grateful to S. Ballandras for the fruitful discussions and design of the single-port resonator.

REFERENCES

[1] P. Defranould and P. Wright, Filtres à ondes de surface, Techniques de lingénieur - Matériaux pour l'électronique et dispositifs associés, Editions T.I., E2200, 2000.

[2] A. Bartasyte, S. Margueron, T. Baron, S. Oliveri, and P. Boulet, Toward high-quality epitaxial $LiNbO_3$ and $LiTaO_3$ thin films for acoustic and optical applications, Adv. Mater. Interfaces 2017, 1600998 and references wherein.

[3] Y. Shibata, K. Kaya, K. Akashi, M. Kanai, T. Kawai, and S. Kawai, "Epitaxial growth and surface acoustic wave properties of lithium niobate films grown by pulsed laser deposition", J. Appl. Phys., vol. 77, p. 1498, .1995

[4] H.K. Lam, J.Y.Dai, and H.L.W Chan, J. Cryst. Growth, vol. 268, p. 144, 2004.

[5] IEEE Standard on Piezoelectricity, ANSI/IEEE Std 176-1987, 1988.

[6] G. Kovacs, M. Anhorn, H.E. Engan, G. Visintini, and C.C.W. Ruppel, "Improved Material Constants for $LiNbO_3$ and $LiTaO_3$" , IEEE IUS, p. 435, 1990

[7] J. Kushibiki, I. Takanaga, S. Komatsuzaki, and T. Ujiie, "Chemical composition dependences of the acoustical physical constants of $LiNbO_3$ and $LiTaO_3$ single crystals," J. Appl. Phys., vol. 91, no. 10, pp. 6341–6349, May 2002.